

Supporting information for:

On the (un)coupling of the chromophore, tongue interactions and overall conformation in *Deinococcus radiodurans* phytochrome

**Heikki Takala<sup>1,2,#,\*</sup>, Heli Lehtivuori<sup>3,#</sup>, Oskar Berntsson<sup>4</sup>, Ashley Hughes<sup>4</sup>, Rahul Nanekar<sup>2</sup>,  
Stephan Niebling<sup>4</sup>, Matthijs Panman<sup>4</sup>, Léocadie Henry<sup>4</sup>, Andreas Menzel<sup>5</sup>, Sebastian Westenhoff<sup>4</sup>,  
and Janne A. Ihalainen<sup>2</sup>**

<sup>1</sup> University of Helsinki, Faculty of Medicine, Anatomy, Helsinki, Finland

<sup>2</sup> University of Jyväskylä, Nanoscience Center, Department of Biological and Environmental Sciences, Jyväskylä, Finland

<sup>3</sup> University of Jyväskylä, Nanoscience Center, Department of Physics, Jyväskylä, Finland

<sup>4</sup> University of Gothenburg, Department of Chemistry and Molecular Biology, Gothenburg, Sweden

<sup>5</sup> Paul Scherrer Institut, 5232 Villigen PSI, 15 Switzerland

Running title: The *(un)coupling of the chromophore and structure in DrBphP*

#These authors contributed equally

\*To whom correspondence should be addressed: Heikki Takala: Faculty of Medicine, University of Helsinki, FI-00014 Helsinki, Finland; E-mail: heikki.takala@helsinki.fi; Tel.: 0358-2941-25238.

## Table of contents

Solution scattering data collection and analysis

Supplementary Figure S1

Supplementary Figure S2

Supplementary Figure S3

References

## Solution scattering data collection and analysis

X-ray solution scattering data was collected at the cSAXS beamline at the Swiss Light Source. The X-ray energy was 11.2 keV and the X-ray beamsize was 100x200  $\mu\text{m}$ . The scattered X-rays were detected by using their SAXS-WAXS dual flight tube and a Pilatus 2M (SAXS) and Pilatus 300k-W (WAXS) detector. The detector was read out at 25 Hz, allowing for 35 ms of X-ray exposure per image. The different samples (ca. 30 mg/ml) were kept still in the X-ray beam in a 1 mm ID quartz capillary. The sample was replenished between X-ray exposures. Two lasers, a red (671 nm) and a far-red (789 nm) were overlapped with the X-ray beam on the capillary. The laser spot size was 300x1000  $\mu\text{m}$  and 1000x1000  $\mu\text{m}$  for the red and far-red laser respectively. The samples were excited using a 10 ms, 671 nm laser pulse (5 mJ/mm<sup>2</sup>) and the Pr state recovered by a 50 ms, 789 nm laser pulse (7 mJ/mm<sup>2</sup>). Every other cycle was without the red laser (dark cycle) and the average of the proceeding and following dark cycle was subtracted from each light cycle to yield difference scattering patterns. Scattering curves deviating from the median in the  $q$ -range  $1.7 < q < 2.2 \text{ \AA}^{-1}$  by more than 5% were considered outliers and were removed before normalization. The absolute scattering curves were normalized to the scattering at  $1.4 < q < 1.6 \text{ \AA}^{-1}$  before calculating differences. The difference scattering signal remains static over the first 0.5 s following red-light exposure and data belonging to these delay times are averaged together. There was no discernible contribution of solvent heating to the scattering signal.

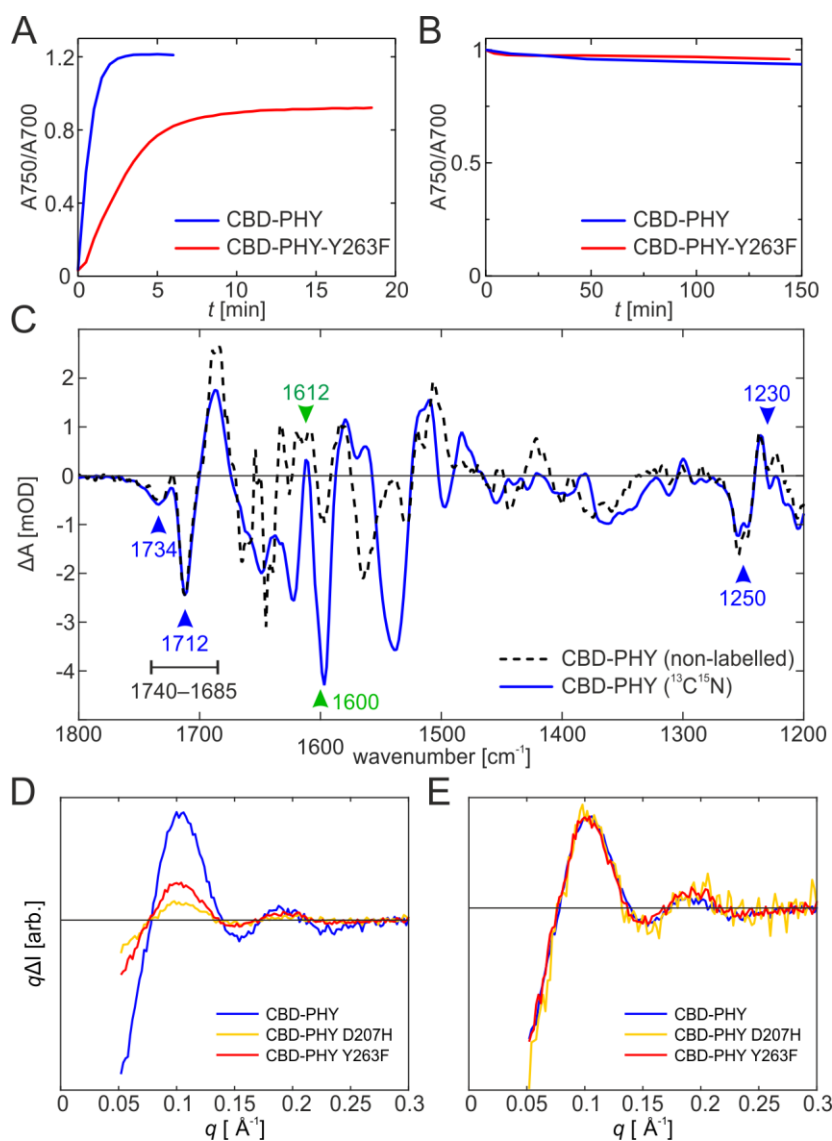


**Figure S1.** Photoconversion and dark reversion rates and FTIR spectra in CBD-PHY variants. (A) The photoconversion rates of the CBD-PHY (blue) and CBD-PHY-Y263F (red) illuminated with  $5 \text{ mW/cm}^2$  light at  $655 \text{ nm}$  wavelength. CBD-PHY reaches the photoequilibrium in 3 minutes, whereas the mutant requires 15 minutes. (B) The dark reversion rates of both variants are similar and very slow. (C) The Pfr–Pr FTIR difference spectra of the non-labeled and  $^{13}\text{C}^{15}\text{N}$ -apoprotein-labeled CBD-PHY samples. The transitions which remain at the same spectral positions regardless of the isotope labeling, e.g. at  $1740\text{--}1685 \text{ cm}^{-1}$ ,  $1250 \text{ cm}^{-1}$ , and  $1230 \text{ cm}^{-1}$  (blue), originate largely from the biliverdin. All vibrations, which involve C or N atoms of the apoprotein are shifted to lower frequency. Note the spectral pattern at  $1600 \text{ cm}^{-1}$  (-) /  $1612 \text{ cm}^{-1}$  (+), which indicates the  $\beta$ -sheet to  $\alpha$ -helix transition (green). A more detailed analysis of the isotope labeled samples are described elsewhere (*unpublished data*). (D-E) The Pfr–Pr difference X-ray scattering signals of wild-type (blue) Y263F (red) and D207H (yellow) scaled to the absolute scattering of each sample (D) or to the positive  $0.1 \text{ \AA}^{-1}$  peak (E).

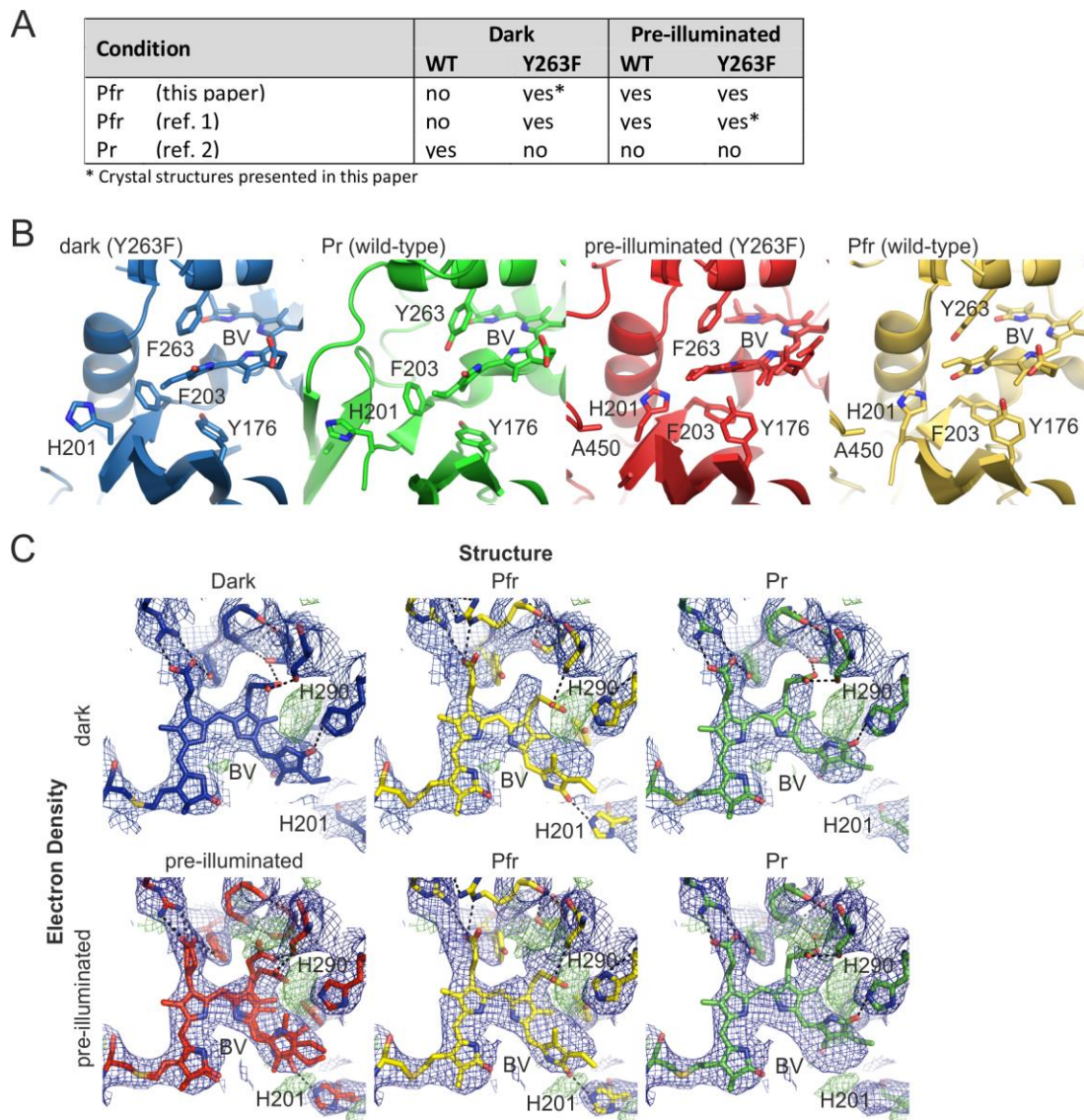


**Figure S2.** Crystallization and chromophore surroundings of the CBD-PHY variants. (A) Crystallization propensities of the wild-type and Y263F in different conditions (1, 2). Pr or Pfr condition means the crystallization condition that favors the corresponding structure. Dark and pre-illuminated indicate the illumination state of the protein crystallized. (B) Structural comparison of the D ring surroundings of CBD-PHY variants. In the dark CBD-PHY-Y263F structure (*blue*), the side chain orientations of Y176, H201 and F203 resemble the Pr structure of the wild-type CBD-PHY (*green*). The pre-illuminated CBD-PHY-Y263F structure (*red*) however resembles the Pfr-state mutant structure of the same fragment (*yellow*). The PDB coordinates 4Q0J (Pr) and 5C5K (Pfr) were used (2, 3). (C) Electron density of dark (upper row) and pre-illuminated (lower row) CBD-PHY-Y263F crystals. The 2Fo-Fc maps are shown as blue mesh; the positive Fo-Fc difference density is shown in green. The existing structures have been aligned to the modelled structures and shown together with our experimental electron densities. The experimental data indicate that dark data support the conformation and interactions of the chromophore in Pr, whereas pre-illuminated electron density can accommodate both Pr and Pfr conformations and interactions. PDB codes of the coordinates used: Pr, 4Q0J (2); Pfr, 5C5K (3). Abbreviations: biliverdin (BV).

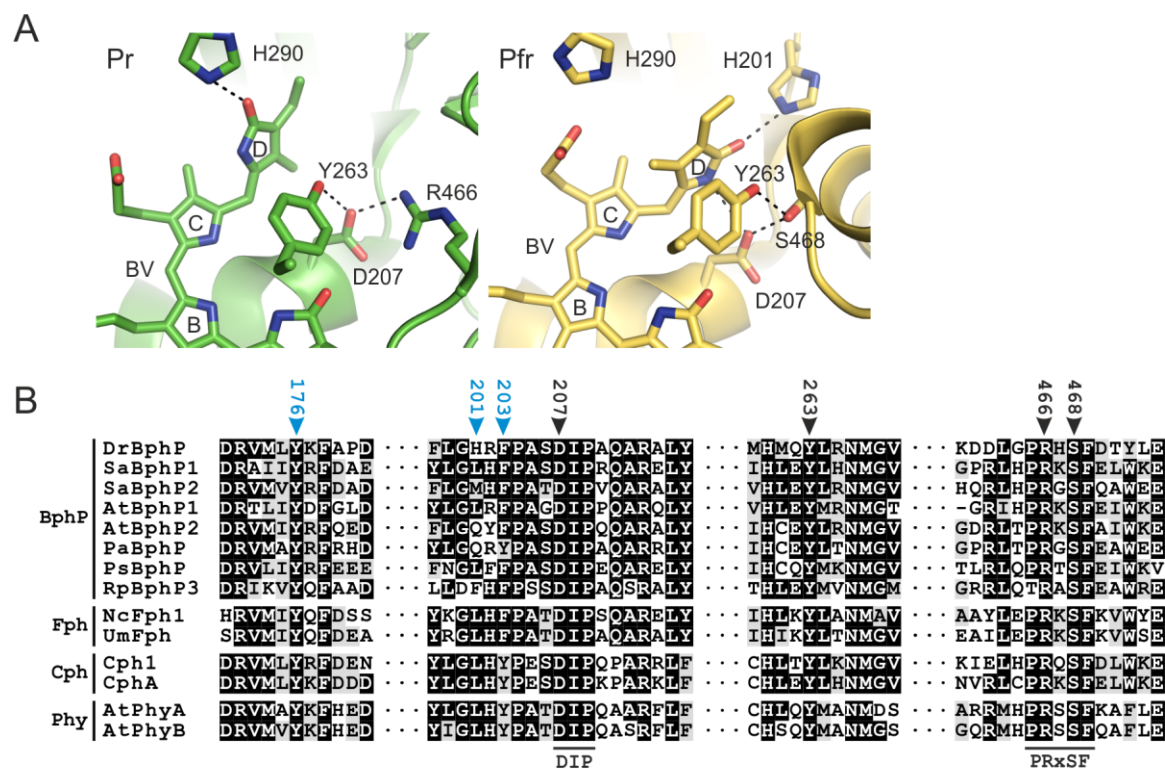


**Figure S3.** Conservation and interactions of selected residues among phytochromes. (A) Structure and interactions of the biliverdin surroundings in Pr (left) and in Pfr state (right). The structures of the *D. radiodurans* CBD-PHY in Pr and Pfr states show two different interaction networks shared by D ring of biliverdin, Y263, and selected residues. Coordinates used for the figure: 4Q0J and 5C5K (2, 3). The modelled waters are not shown; biliverdin (BV) and selected residues are shown as sticks. (B) Partial sequence alignment of selected bacterial (BphP), fungal (Fph), cyanobacterial (Cph), and plant phytochromes (Phy). The residues of interest are indicated and numbered according to DrBphP. Residues are color-coded according to the extent of conservation (black, highly conserved; white non-conserved). DrBphP (*Deinococcus radiodurans* R1), SaBphP1 and P2 (*Stigmatella aurantiaca* DW4/3-1), AtBphP1 and P2 (*Agrobacterium tumefaciens* C58), PaBphP (*Pseudomonas aeruginosa* PAO1), PsBphP (*Pseudomonas syringae* pv. tomato T1), RpBphP3 (*Rhodopseudomonas palustris* TIE-1), NcFph1 (*Neurospora crassa*), UmFph (*Ustilago maydis* 521), Cph1 (*Synechocystis* sp. PCC6803), CphA (*Nostoc* sp. PCC7120), AtPhyA and AtPhyB (*Arabidopsis thaliana*). The sequence alignment was generated with Clustal Omega (version 1.2.1) and processed with BOXSHADE as previously (4).

## References

1. Takala, H., Björling, A., Berntsson, O., Lehtivuori, H., Niebling, S., Hoernke, M., Kosheleva, I., Henning, R., Menzel, A., Ihalainen, J.A., and Westenhoff, S. (2014) Signal amplification and transduction in phytochrome photosensors. *Nature*. **509**, 245-248
2. Burgie, E.S., Wang, T., Bussell, A.N., Walker, J.M., Li, H., and Vierstra, R.D. (2014) Crystallographic and Electron Microscopic Analyses of a Bacterial Phytochrome Reveal Local and Global Rearrangements During Photoconversion. *J.Biol.Chem.* 289, 24573-24587
3. Burgie, E.S., Zhang, J., and Vierstra, R.D. (2016) Crystal Structure of Deinococcus Phytochrome in the Photoactivated State Reveals a Cascade of Structural Rearrangements during Photoconversion. *Structure*. 24, 448-457
4. Björling, A., Berntsson, O., Takala, H., Gallagher, K.D., Patel, H., Gustavsson, E., St Peter, R., Duong, P., Nugent, A., Zhang, F., Berntsen, P., Appio, R., Rajkovic, I., Lehtivuori, H., Panman, M.R., Hoernke, M., Niebling, S., Harimoorthy, R., Lamparter, T., Stojkovic, E.A., Ihalainen, J.A., and Westenhoff, S. (2015) Ubiquitous Structural Signaling in Bacterial Phytochromes. *J.Phys.Chem.Lett.* 3379-3383